Fortschr. Phys. **49** (2001) 10–11, 1071–1076

Quantum Zeno Tomography

S. PASCAZIO[1,2]), P. FACCHI[1,2]), Z. HRADIL[3]), G. KRENN[1]), and J. ŘEHÁČEK[3])

[1]) Dipartimento di Fisica, Università di Bari, I-70126 Bari, Italy
[2]) Istituto Nazionale di Fisica Nucleare, Sezione di Bari, I-70126 Bari, Italy
[3]) Department of Optics, Palacký University, 17. listopadu 50, 772 00 Olomouc, Czech Republic

Abstract

We discuss the possibility of devising a tomographic scheme that makes use of the quantum Zeno effect. We show that such a method works better than the standard one, provided that the different levels of "gray" in the sample are not uniformly distributed.

PACS: 03.65.Xp

1. Introduction

The quantum Zeno effect (QZE) consists in the hindrance of the evolution of a quantum system due to frequent measurements [1]. This phenomenon has been widely investigated during the last few years, not only because of its intrinsic interest, but also for its potential applications. We discuss here a remarkable application in tomography. In an ordinary tomographic setup one measures the attenuation of a beam of particles passing through a sample and endeavors to infer the absorption coefficient (density) of the sample in the beam section. The resolution is limited by two main factors: noise (beam intensity fluctuations) and damage provoked by the radiation absorbed by the sample. In a recent paper [2] we have discussed the possibility of carrying out "absorption-free" tomography by making use of the QZE. Our proposal is related to other interesting work [3]. We review here our main ideas.

2. Black, White and Gray Objects

Consider the Mach-Zender interferometer (MZI) with "feedback" shown in Fig. 1(a). A semitransparent object, whose transmission amplitude is τ (assumed real for simplicity) is placed in the lower arm of the interferometer. The particle emitted by the source S is initially (at time $t = t_{\text{in}}$) injected from the left, crosses the interferometer L times and is finally (at $t = t_{\text{fin}}$) detected by one of two detectors D. The two semitransparent mirrors M are identical and their transmission and reflection coefficients are

$$c \equiv \cos\theta_L\,, \qquad s \equiv \sin\theta_L\,, \qquad (\theta_L = \pi/4L) \tag{1}$$

respectively. Both coefficients depend on L, the number of "loops" in the MZI. Let

$$\begin{pmatrix}1\\0\end{pmatrix} = |\text{Zeno}\rangle\,, \qquad \begin{pmatrix}0\\1\end{pmatrix} = |\text{orthogonal}\rangle \tag{2}$$

 0015-8208/01/10-1111-1071 $ 17.50+.50/0

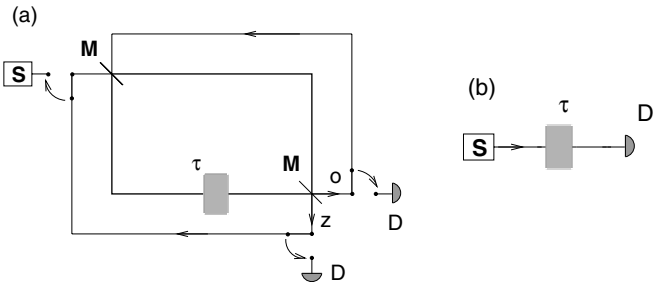

Fig. 1. Comparison between the Zeno interferometric setup (a) and the standard transmission experiment (b). A sample whose transmission amplitude is τ is analyzed in both cases. S = source, M = semitransparent mirror, D = detector; o (z) denotes the orthogonal (Zeno) channel

be the extraordinary and ordinary channels of the MZI, respectively. We take the incoming state of the particle to be $|\text{in}\rangle = |\text{Zeno}\rangle = \binom{1}{0}$. The total effect of one "loop" in the MZI is

$$V_\tau = BAB\,, \qquad B = \begin{pmatrix} c & -s \\ s & c \end{pmatrix}, \qquad A = \begin{pmatrix} 1 & 0 \\ 0 & \tau \end{pmatrix}. \tag{3}$$

Notice that A is not unitary: if $\tau < 1$ there is a probability loss. The angle θ_L is chosen so that if $\tau = 1$ ("white" object in the lower arm of the MZI) the particle ends up in the "orthogonal" channel:

$$|\text{out}\rangle = V_{\tau=1}^L |\text{in}\rangle = |\text{orthogonal}\rangle\,. \qquad (\forall L) \tag{4}$$

On the other hand, if $\tau = 0$ ("black" object in the lower arm of the MZI), we readily obtain

$$|\text{out}\rangle = \lim_{L\to\infty} V_{\tau=0}^L\, |\text{in}\rangle = |\text{Zeno}\rangle\,. \tag{5}$$

In the infinite L limit the particle ends up in the "Zeno" channel (QZE). A classical measuring apparatus (here the black sample), placed in one arm of the interferometer, projects the illuminating particle into the other arm, destroying interference, freezing the evolution and forcing the particle to exit through a different channel from that it would have chosen had both arms been transparent (white sample). Equations (4) and (5) express the remarkable result that "white" and "black" objects can be discriminated with unit probability *without* any photon absorption by the sample. This is, in essence, a straightforward consequence of QZE.

In practical applications, however, samples are normally neither black nor white: they are *gray*. We are therefore interested in understanding what happens for $0 < \tau < 1$ [4]. The computation of V_τ^L is straightforward but lengthy [2] and yields

$$|\text{out}\rangle = \lim_{L\to\infty} V_\tau^L\, |\text{in}\rangle = |\text{Zeno}\rangle\,, \qquad \tau \neq 1\,. \tag{6}$$

This shows that even for a semitransparent object, with transmission coefficient $\tau \neq 1$, a *bona fide* QZE takes place and the particle ends up in the Zeno channel with probability one.

This interesting result, however, does not solve the problem of *distinguishing* different values of τ (different "shades" or "levels" of gray). This is not a simple task, for after a very large number of loops L the particle ends up in the orthogonal channel only if $\tau = 1$ [see (4)]; by contrast, for any value of $\tau \neq 1$, the particle ends up in the Zeno channel [see (6)] *irrespectively* of the particular value of τ. However, the asymptotic corrections in V_τ^L

do depend on τ. One can show that the final state of the particle after $L(\gg 1)$ loops in the MZI reads

$$V_\tau^L \begin{pmatrix} 1 \\ 0 \end{pmatrix} = \begin{pmatrix} u_z \\ u_o \end{pmatrix} = \begin{pmatrix} 1 - \dfrac{\pi^2}{8L} \dfrac{1+\tau}{1-\tau} + O(L^{-2}) \\ O(L^{-1}) \end{pmatrix}, \tag{7}$$

where u_z and u_o are the (real) amplitudes in the Zeno and orthogonal channels, respectively. By exploiting this feature, we shall show in Sec. 3 that it is indeed possible to resolve different gray levels by QZE, within a given statistical accuracy. Let $(0 \le \tau < 1)$

$$\begin{aligned} p_z(\tau) &= u_z^2 = 1 - \frac{\pi^2}{4L} \frac{1+\tau}{1-\tau} + O(L^{-2}), \qquad p_0(\tau) = u_o^2 = O(L^{-2}), \\ p_a(\tau) &= 1 - p_z(\tau) - p_0(\tau) = \frac{\pi^2}{4L} \frac{1+\tau}{1-\tau} + O(L^{-2}) \end{aligned} \tag{8}$$

be the probabilities that the particle is detected in the Zeno, orthogonal channel or is absorbed by the semitransparent object, respectively. We assume that a fixed number of particles N is sent in the MZI during an experimental run. In this situation the distribution of particles in the Zeno, orthogonal or absorption channels follows a multinomial statistics with probabilities (8). However, by increasing the number of loops L, p_o vanishes much faster than p_a, so that for large L the distribution becomes in practice binomial with $p_a + p_z \approx 1$. (Since p_a is also small in this limit, the detection statistics is effectively Poissonian.)

Notice that, if one performs a standard transmission experiment, like in Fig. 1(b), the statistics is again binomial, with detection and absorption probabilities

$$p'_d(\tau) = \tau^2, \qquad p'_a(\tau) = 1 - \tau^2. \tag{9}$$

3. Statistics

The goal of a "Zeno tomography" is to get information about the distribution of the absorption coefficient in the sample, absorbing as few particles as possible. Let us first assume that all levels of gray are uniformly distributed in the sample (i.e. τ is continuously distributed between 0 and 1) and let us try to estimate τ^2 from the counted number of particles, absorbing as few particles as possible for the requested precision. To perform this task in an optimal way one should find optimal estimators for each scheme. A lower bound on the variance of an unbiased estimator $\hat{T}$ of the parameter T (here $T = \tau^2$) is the Cramér-Rao lower bound (CRLB) [5],

$$(\Delta \hat{T})^2 \ge \frac{1}{F} \equiv \left\langle \left[\frac{\partial}{\partial T} \ln p(n \mid T) \right]^2 \right\rangle^{-1}, \tag{10}$$

where F is the Fisher information, $p(n \mid T)$ the probability of observing n particles conditioned by the value T of the unknown parameter and $\langle \ldots \rangle$ denotes ensemble average with respect to n. In both cases (9) and (8) the probability p is binomially distributed and yields

$$(\Delta \hat{T}_{\mathrm{st}})^2 \ge \frac{\tau^2(1-\tau^2)}{N}, \qquad (\Delta \hat{T}_{\mathrm{Ze}})^2 \ge \frac{4\tau^2(1-\tau)^3\,(1+\tau)\,L}{\pi^2 N} \tag{11}$$

for standard and Zeno tomography, respectively, N being the (fixed) number of input particles in both cases. Expressing the above inequalities in terms of the number of *absorbed* particles $N_a^{(\mathrm{st})} = Np'_a$ and $N_a^{(\mathrm{Ze})} = Np_a$, they both reduce to the same bound

$$\Delta\hat{T}_{\mathrm{st,Ze}} \geq \Delta\hat{T}^{\mathrm{opt}}_{\mathrm{st,Ze}} = \frac{\tau(1-\tau^2)}{\sqrt{N_a^{(\mathrm{st}),\,(\mathrm{Ze})}}}\,, \tag{12}$$

showing that the CRLB's for standard and Zeno tomography are the same, *given* the number of absorbed particles. Furthermore, it is trivial to show that the unbiased estimator given by the relative frequency of transmitted particles in the standard setup, $\hat{T}_{\mathrm{st}} = n_t/N$, saturates the CRLB (12). Hence the Zeno estimation can be at best as good as the standard one: it cannot be better. This is bad news.

In spite of this result, we now show that Zeno performs better when one wants to distinguish two levels of gray that are not equally populated in the sample. This is good news, for it enables one to find a method that in some cases works better than the standard one. The fundamental observation is that $p_a(\tau)$ in (8), unlike $p'_a(\tau)$ in (9), is an *increasing* function of τ. Therefore, with respect to absorbed particles, the Zeno tomographic image (for sufficiently large L) yields a kind of negative of the standard absorption tomographic image: denser samples absorb fewer particles. Indeed, the absorption probability in (8) reduces to the same form as the standard one (9) by introducing an "effective" transmission coefficient $\tau^{\mathrm{Ze}}_{\mathrm{eff}} = \sqrt{1-p_a}$. For example, if we take $\tau_1 = 0.98$, $\tau_2 = 0.99$ and choose $L = 12000$, then, according to Eq. (8), we get $\tau^{\mathrm{Ze}}_{\mathrm{eff}1} \approx 0.99$ and $\tau^{\mathrm{Ze}}_{\mathrm{eff}2} \approx 0.98$. The two gray levels are *interchanged* by the Zeno apparatus. If most of the sample has transmission coefficient τ_2 the absorbed energy is reduced by using the Zeno setup!

A more precise comparison of the performances of the Zeno and standard techniques can be given in the framework of decision theory. For simplicity let us focus on distinguishing only two gray levels τ_1 and τ_2 ($\tau_1 < \tau_2$) corresponding to hypotheses H_1 and H_2 that occur in the sample with frequencies $P_0(H_1) = \alpha$ and $P_0(H_2) = 1-\alpha$. Since both experiments obey the same statistics we use the notation of the Zeno experiment. The decision is based on the number of absorbed particles n_a: if n_a is smaller than or equal to a decision level n_d, H_1 is chosen; otherwise H_2 is chosen. The probability of making an error in identifying the gray level of a given pixel is

$$P_e = \alpha P(H_2 \mid H_1) + (1-\alpha)\,P(H_1 \mid H_2) \tag{13}$$

($P(H_i \mid H_j)$ being the probability of choosing hypothesis H_i when H_j is true), where

$$P(H_1 \mid H_2) = \sum_{n_a \leq n_d} p(n_a \mid H_2)\,, \qquad P(H_2 \mid H_1) = \sum_{n_a > n_d} p(n_a \mid H_1) \tag{14}$$

and

$$p(n_a \mid H_j) = \binom{N}{n_a} p_a(\tau_j)^{n_a}\,[1-p_a(\tau_j)]^{N-n_a}\,, \tag{15}$$

is the binomial probability of absorbing n_a particles when H_j is true. An optimal protocol is given by determining n_d that minimizes the error (13). Alternatively, one determines the optimum n_d by solving for

$$\text{Likelihood} = \mathcal{L} = \frac{p(n_a \mid H_1)\,P_0(H_1)}{p(n_a \mid H_2)\,P_0(H_2)} = \frac{\alpha p(n_a \mid H_1)}{(1-\alpha)\,p(n_a \mid H_2)} = 1\,. \tag{16}$$

The likelihood criterion (16) is also valid for other (non binomial) statistics and can be easily generalized to the case of more than two gray levels. Interestingly, the likelihood method (16) and the minimization of the error probability (13) leads to the *same* conclusion [this might be a fluke of our (simplifying) choice of discriminating between two levels of gray only]. In both cases one gets

$$n_d = \frac{\log\left[\dfrac{1-\alpha}{\alpha}\right] - N\log\left[\dfrac{1-p_a(\tau_1)}{1-p_a(\tau_2)}\right]}{\log\left[\dfrac{p_a(\tau_1)}{p_a(\tau_2)}\right] - \log\left[\dfrac{1-p_a(\tau_1)}{1-p_a(\tau_2)}\right]} \tag{17}$$

and, substituting in (13),

$$\begin{aligned} P_e = {} & \alpha\{1 - B_I[N - \tilde{n}_d, 1 + \tilde{n}_d; 1 - p_a(\tau_1)]\} \\ & + (1-\alpha)\, B_I[N - \tilde{n}_d, 1 + \tilde{n}_d; 1 - p_a(\tau_2)]\,, \end{aligned} \tag{18}$$

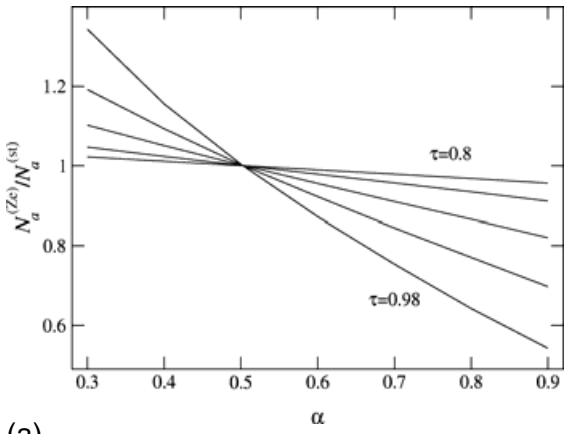

(a)

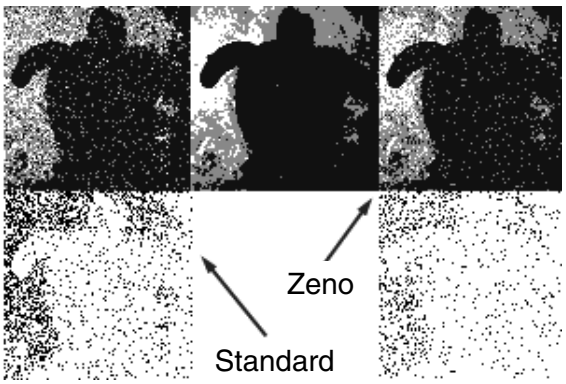

(b)

Fig. 2. (a) Ratio of the number of absorbed particles in the Zeno ($N_a^{(\mathrm{Ze})}$) and standard ($N_a^{(\mathrm{st})}$) setup. $P_e = 1.5\%$; $d\tau = 0.01$; $\tau = \{0.8, 0.9, 0.95, 0.97, 0.98\}$. (b) Comparison of standard and Zeno tomographic techniques. The original object (a turtle, center) consists of three levels of gray $\tau_1 = 0.99$, $\tau_2 = 0.98$ and $\tau_3 = 0.92$, occurring with relative frequencies $f_1 = 0.1$, $f_2 = 0.2$ and $f_3 = 0.7$, respectively. We fixed N_a so that about 4.3 particles per pixel are absorbed on the average in both cases and chose $L = 12,000$ loops for the Zeno reconstruction. The reconstructed objects (above) and misinterpreted pixels (below) are shown for standard (left) and Zeno (right) tomography. The number of misinterpreted pixels is *half* for the Zeno reconstruction.

where $B_I(a,b;z)$ is the regularized incomplete Beta function [6] and $\tilde{n}_d$ is the greatest integer less than or equal to n_d. The mean number of absorbed particles is

$$N_a^{(\mathrm{Ze})} = N[\alpha p_a(\tau_1) + (1-\alpha)\, p_a(\tau_2)]\,. \tag{19}$$

Using Eqs. (17) and (19), the average probability of error (18) can be expressed as a function of α, $\tau \equiv \tau_1$, $d\tau = \tau_2 - \tau_1$ and $N_a^{(\mathrm{Ze})}$. The probability of error for the standard setup is obtained in a completely analogous way.

The performances of the Zeno and standard methods are compared in Fig. 2(a). The number of absorbed particles has been calculated by solving numerically Eqs. (17)−(19), while keeping the mean error P_e constant. Their ratio is shown as a function of α for a few values of the transmission coefficient τ. Notice that there is *no* improvement for two equally frequent levels of gray. On the other hand the exposition of the sample can be significantly reduced if the distribution of gray levels in the sample is not uniform.

The results of a numerical simulation are shown in Fig. 2(b). The sample is a turtle (a tribute to Zeno!) with 3 levels of gray. The original is at the center, the reconstructed images with the Zeno and standard method are above, at the left and right, respectively. Below there are the pixels that have been misinterpreted. For the same number of absorbed particles, provided the object contains a small fraction of more transparent pixels and a larger fraction of more absorbing material, the number of misinterpreted pixels is *half* for the Zeno reconstruction. This proves that quantum Zeno tomography performs better than standard tomography if a given prior knowledge about the distribution of grays in the sample is available. This is a common situation in radiography, where one is often interested in detecting a small structure in a uniform background.

Acknowledgement

This paper is dedicated to Professor Jan Peřina on the occasion of his 65th birthday. This work is supported by the TMR-Network of the European Union "Perfect Crystal Neutron Optics" ERB-FMRX-CT96-0057. J.R. and Z.H. acknowledge support by the project LN00A015.

References

[1] B. MISRA and E. C. G. SUDARSHAN, J. Math. Phys. **18** (1977) 756; S. PASCAZIO, M. NAMIKI, G. BADUREK, and H. RAUCH, Phys. Lett. **A179** (1993) 155. For a review, see H. NAKAZATO, M. NAMIKI, and S. PASCAZIO, Int. J. Mod. Phys. **B10** (1996) 247; D. HOME and M. A. B. WHITAKER, Ann. Phys. **258** (1997) 237; P. FACCHI and S. PASCAZIO, in: Progress in Optics **42**, Edited by E. Wolf, Elsevier Amsterdam, 2001.

[2] P. FACCHI, Z. HRADIL, G. KRENN, S. PASCAZIO, and J. ŘEHÁČEK, Towards a quantum Zeno tomography, quant-ph/0104021.

[3] R. H. DICKE, Am. J. Phys. **49** (1981) 925; Found. Phys. **16** (1986) 107; A. C. ELITZUR and L. VAIDMAN, Found. Phys. **23** (1993) 987; M. HAFNER and J. SUMMHAMMER, Phys. Lett. **235A** (1997) 563; P. KWIAT, H. WEINFURTER, T. HERZOG, A. ZEILINGER, and M. KASEVICH, Phys. Rev. Lett. **74** (1995) 4763.

[4] G. KRENN, J. SUMMHAMMER, and K. SVOZIL, Phys. Rev. **A61** (2000) 052102; G. MITCHINSON and S. MASSAR, Phys. Rev. **A63** (2001) 032105.

[5] C. R. RAO, Bull. Calcutta Math. Soc. **37** (1945) 81; H. CRAMÉR, Mathematical methods of statistics, Princeton University Press, 1946.

[6] M. ABRAMOVITZ and I. A. STEGUN, *Handbook of mathematical functions*, Dover, New York, 1972, 26.5.1 and 26.5.7.